

## Research Article

# Template-Free Preparation and Photocatalytic and Photoluminescent Properties of Brookite TiO<sub>2</sub> Hollow Spheres

Yunjian Wang  and Yuchan Li

Anhui Key Laboratory of Energetic Materials, College of Chemistry and Materials Science, Huaibei Normal University, Huaibei, 235000 Anhui, China

Correspondence should be addressed to Yunjian Wang; wangyunjianmail@163.com

Received 24 December 2018; Accepted 19 February 2019; Published 25 March 2019

Guest Editor: Zhen Yu

Copyright © 2019 Yunjian Wang and Yuchan Li. This is an open access article distributed under the Creative Commons Attribution License, which permits unrestricted use, distribution, and reproduction in any medium, provided the original work is properly cited.

The preparation of high-purity brookite TiO<sub>2</sub> with a unique morphology is rare and difficult. Herein, high-purity brookite TiO<sub>2</sub> hollow spheres were hydrothermally synthesized by employing titanium sulfate as the titanium source and chloroacetic acid and sodium hydroxide as the pH regulator. The structure, morphology, and optical properties were characterized by X-ray diffraction (XRD), scanning electron microscopy (SEM), transmission electron microscopy (TEM), X-ray photoelectron spectroscopy (XPS), and UV-Vis diffuse reflectance spectroscopy (UV-Vis DRS). The results showed that the as-prepared brookite TiO<sub>2</sub> exhibited a hollow-sphere morphology with a size of about 1.0 micrometer and showed a direct band gap of 3.13 eV. Additionally, thermal analysis in combination with infrared spectroscopy showed that the as-prepared brookite TiO<sub>2</sub> was surface capped by water and organic molecules. Finally, the photocatalytic and photoluminescent properties of brookite TiO<sub>2</sub> were studied.

## 1. Introduction

The control of TiO<sub>2</sub> polymorphs and morphology has attracted enormous interest due to its fascinating structure and shape-dependent physicochemical properties [1–3]. As a popular photocatalyst, TiO<sub>2</sub> contains three common polymorphs: anatase, rutile, and brookite [4, 5]. All three polymorphs are constructed by the different connections of the distorted TiO<sub>6</sub> octahedra. Among these polymorphs, the preparation and properties of both anatase and rutile are intensively studied [6, 7]. Alternatively, the report on TiO<sub>2</sub> in the brookite form is rare for a lack of understanding of its properties and synthetic approach [8]. In this regard, Lin et al. report the first breakthrough in the synthesis of a brookite TiO<sub>2</sub> nanosheet with an excellent photocatalytic performance through a spatial charge transfer control with specific crystal surface exposure [9]. Since then, a growing number of methods are emerging to explore the unique morphology-dependent property of brookite TiO<sub>2</sub>. For

example, Choi and Yong report the facile hydrothermal preparation of brookite nanoarrays using an environmentally benign one-step reaction [10]. Just like nitrogen-doped anatase or rutile, nitrogen-doped brookite TiO<sub>2</sub> with enhanced visible-light photoactivity is also reported by Pan and Jiang [11]. Although numerous synthetic strategies have been developed for the fabrication of the brookite phase, the phase-formation mechanism of a brookite polymorph is still under controversy, and it still remains the least studied TiO<sub>2</sub> photocatalyst due to the difficulties usually encountered in obtaining it as a pure phase [12]. Although it is exceedingly difficult to explore a novel approach, it is still of great interest to synthesize pure brookite with a unique morphology for its great potential in applications ranging from solar cells and sensors to photocatalysis [13–15]. Herein, we report the first fabrication of pure brookite hollow spheres through the self-assembly of nanoblocks under a facile hydrothermal condition, and we report brookite's structure, surface, and photocatalytic properties as well.

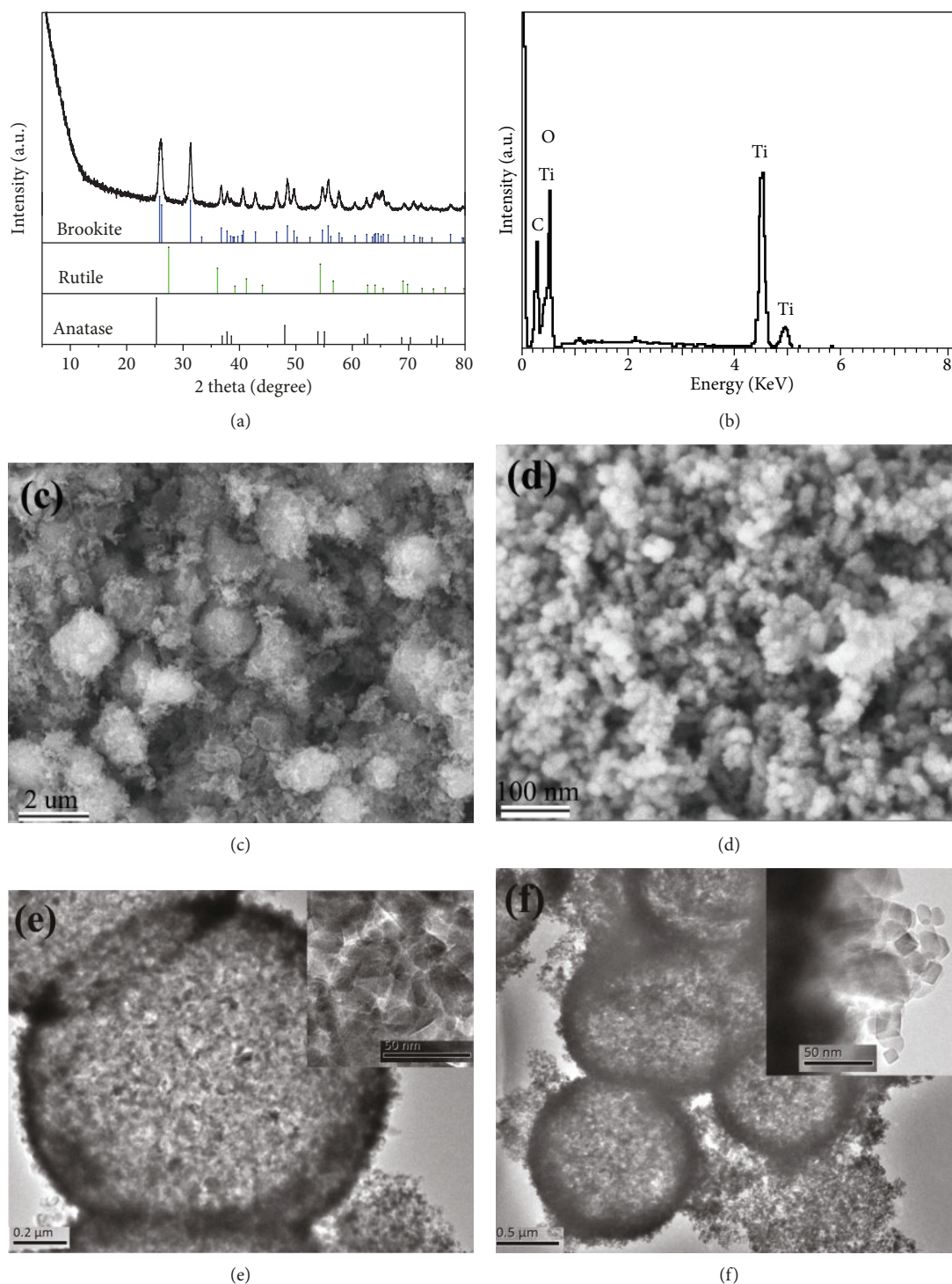


FIGURE 1: (a) XRD pattern, (b) EDS spectrum, and (c, d) SEM and (e, f) TEM images of the sample.

## 2. Experimental

**2.1. Materials.** All reagents were purchased from Sinopharm Chemical Reagent Co. Ltd., Shanghai, China. All reagents were of analytical purity and used without further purification.

**2.2. Sample Preparation.** The brookite  $\text{TiO}_2$  sample was prepared under a typical hydrothermal condition as follows: 2.6301 g titanium sulfate was dissolved in 30 mL distilled

water under constant stirring; then, 5.0 g chloroacetic acid, 2.125 g NaOH, and 15.012 g carbamide were added into the above solution and stirred for 2 h until the solution became a translucent yellow; then, the solution was transferred to a 100 mL Teflon-lined stainless steel autoclave that was allowed to react at 200°C for 9 h. The product was centrifuged and washed with deionized water for three times and then dried at 80°C for 12 h.

**2.3. Sample Characterization.** XRD analysis was performed on a Bruker D8 ADVANCE X-ray powder diffractometer equipped with Cu K $\alpha$  radiation. The morphology of the sample was observed by FE-SEM (JEOL JSM-6700) and TEM (JEM-2010). The infrared spectrum of the sample was measured on a PerkinElmer IR spectrophotometer using a KBr pellet technique. TG-DTA was measured on a NETZSCH STA 449C apparatus. Optical diffuse reflectance spectra of the samples were measured using a Lambda 900 UV-Vis spectrometer. The valence states were studied by XPS employing an ESCALAB MKII spectrometer from VG Scientific Co., with an Al K $\alpha$  (1486.6 eV) line at 150 W. The photocatalytic activities were evaluated by the degradation of 10 ppm methyl orange (MO) in an aqueous solution under ultraviolet radiation. The photoluminescence spectrum was measured on a Cray Eclipse fluorescence spectrophotometer with a Xe lamp excited at 310 nm and recorded at a scan rate of 120 nm·min<sup>-1</sup>.

### 3. Results and Discussion

Figure 1(a) shows the XRD pattern of the hydrothermally prepared TiO<sub>2</sub> sample at 200°C for 9 h. It is seen that the peak which appeared at  $2\theta = 30.8^\circ$  is the diffraction peak from the (121) crystal plane of brookite, which is a characteristic of a brookite polymorph. The diffraction peak of rutile was not observed. It should be noted that anatase has almost the same diffraction peaks of brookite except for the diffraction peaks of the (121) crystal plane. For the mixture of rutile and brookite, the phase content of brookite can be estimated from the relative intensity of their diffraction peak. Based on previous literature, the phase purity of brookite was evaluated up to 99.8% by the intensity ratio of diffraction peaks using the following formula:  $I_{121}^{\text{brookite}} / (I_{120}^{\text{brookite}} + I_{101}^{\text{anatase}})$  [16]. EDS analysis in Figure 1(b) shows that the sample is composed of Ti and O elements with a small amount of carbon, which might come from the surface-adsorbed organics. The surface morphology and size of the sample was investigated by SEM, as displayed in Figures 1(c) and 1(d). The brookite TiO<sub>2</sub> presents irregular spheres with sizes ranging from 1 to 2  $\mu\text{m}$ . The internal structure of the spheres was further examined by TEM, as shown in Figures 1(e) and 1(f). The brookite sphere has a hollow structure, assembled by nanoblocks of 20 nm in size. The inserts in Figures 1(e) and 1(f) show the surface structure of the hollow sphere. Figure 2 shows the XRD patterns of the samples prepared for different periods of hydrothermal reaction time. It is observed that the sample formed at the early stage of 1 h is the mixture of anatase and a small amount of brookite. It is interesting to find that anatase gradually transformed into brookite form with the increase of reaction time, and high-purity brookite was obtained by extending the reaction time to 9 hours. The anatase-to-brookite phase transition can be seen from the change of diffraction peak intensity from brookite, as indicated by the arrows in Figure 2. The crystalline size increased during the phase-transition process, which conforms with the popular opinion that anatase TiO<sub>2</sub> is stable in small sizes while brookite is more stable in big sizes [17].

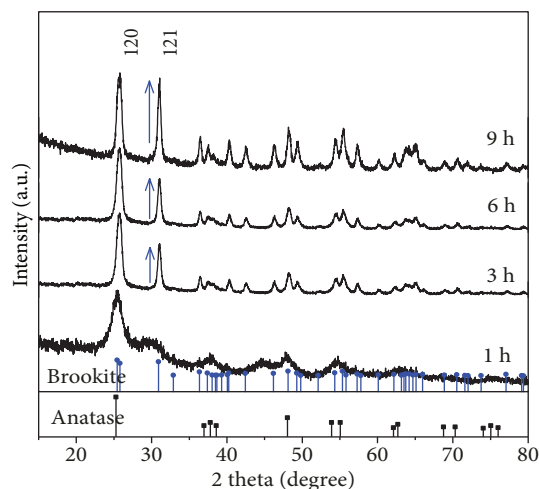


FIGURE 2: XRD patterns of the samples prepared at given periods of time. (The arrow points out the intensity of the (121) diffraction peak from brookite which increases with time.)

The thermal stability of the as-prepared brookite TiO<sub>2</sub> was investigated by TG-DTA, as shown in Figure 3(a). Apparently, about 3.5 wt.% weight loss below 400°C was attributed to the vaporization of the water molecules that existed on the surface of the sample [18], which was further suggested by the wide endothermic peak in this temperature range. In the temperature range from 400 to 800°C, an obvious 16.8 wt.% weight loss in the TGA curve accompanied with a sharp exothermic peak in the DTA curve was observed, which may be attributed to the combustion of surface-adsorbed organic matter in an air atmosphere [19]. It is noted that the DTA curve exhibits another strong endothermic peak at around 900°C despite that no significant weight loss was observed on the TGA curve in this temperature range, corresponding to the polymorph transition from metastable brookite to stable rutile. In previous literature reported by Xu et al. [20], brookite-to-rutile phase-transition temperature was fixed at 850°C as detected by in situ high-temperature XRD. By comparison, this phase-transition temperature observed in our work is a little higher, and it may be related to the hollow structure of brookite. To further investigate the surface-adsorbed species, the FT-IR spectrum of the brookite sample was measured in the wavenumber range 400–4000 cm<sup>-1</sup>. The strongest band located at 3458 cm<sup>-1</sup> is attributed to the vibration of H-O bonds for surface adsorption, and the weak absorption centered at 1645 cm<sup>-1</sup> is associated with the deformation vibration of H-O bonds from the surface adsorption layers [21]. Several bands at 422, 484, 560, and 728 cm<sup>-1</sup> in the low wavenumber range are the characteristic absorption peaks of brookite TiO<sub>2</sub> [22]. From the UV-Vis absorption spectrum in Figure 3(c), the absorption edge was found to be around 387.2 nm for the hollow-structure brookite. It is generally believed that the brookite-structure TiO<sub>2</sub> belongs to an indirect-type semiconductor [9, 23]. The corresponding bandgap energy is estimated as follows:

$$\alpha = \frac{K(h\nu - E_g)^{1/n}}{h\nu}, \quad (1)$$

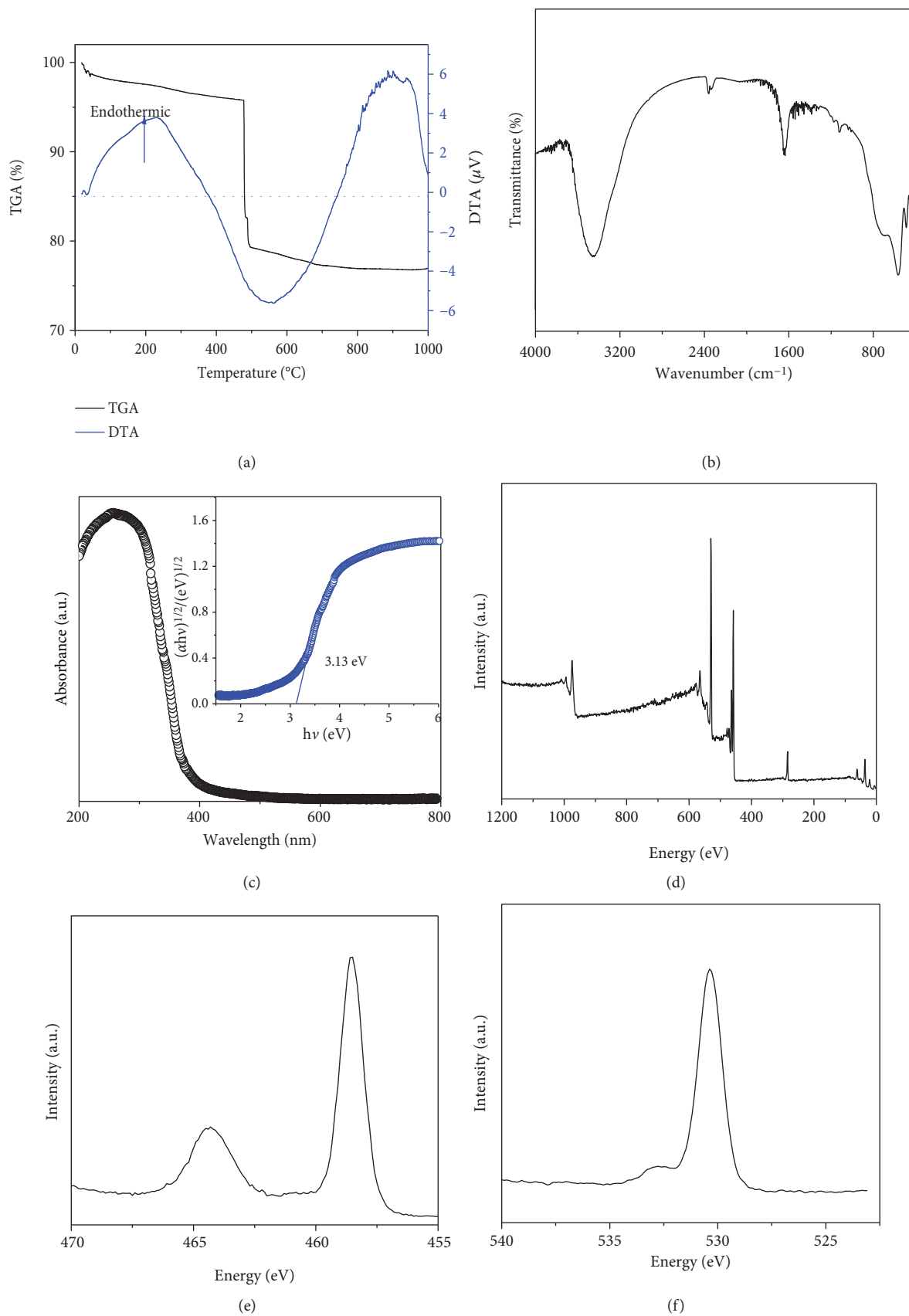


FIGURE 3: (a) TG-DTA curves, (b) FT-IR spectrum, and (c) UV-visible diffusion reflectance spectrum. Insert shows the energy dependence of  $(\alpha h\nu)^2$  for the sample. (d) XPS survey spectrum and high-resolution XPS spectrum for O 1s (e) and Ti 2p (f) of the sample.

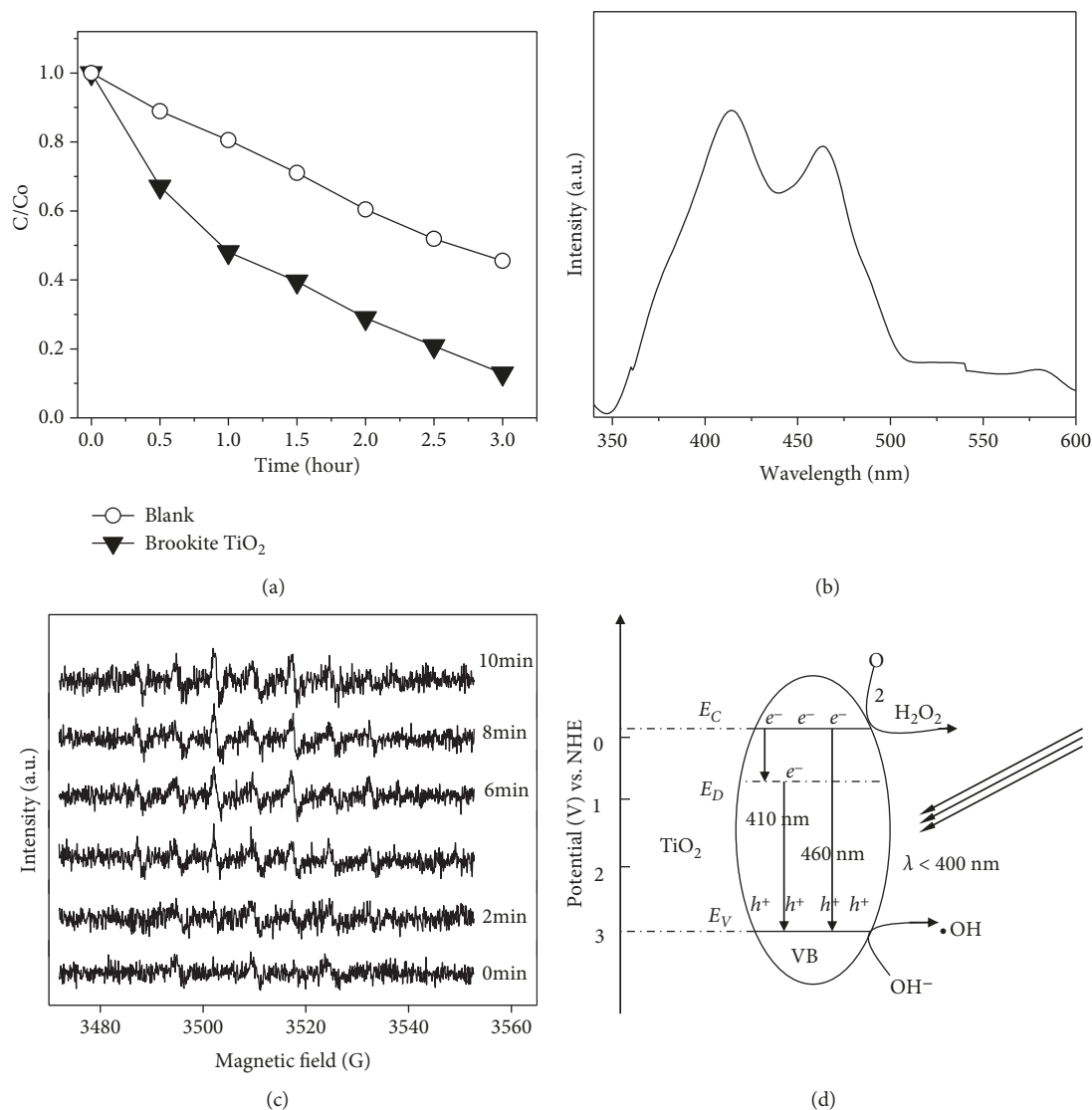


FIGURE 4: (a) Photocatalytic performance of MO degradation, (b) photoluminescence emission spectrum excited at 310 nm, (c) time-varied ESR spectra for DMPO-OH, and (d) schematic diagram for the photochemical process for TiO<sub>2</sub> hollow spheres.

where  $\alpha$  is absorbance,  $h\nu$  represents the energy of incident photons,  $K$  is a constant, and  $n$  equals to 2 for direct transition and 1/2 for indirect transition [24]. As displayed in the insert of Figure 3(c), the bandgap energy  $E_g$  was 3.13 eV for the prepared hollow-structure brookite TiO<sub>2</sub>, in good agreement with previously reported results [25]. The surface chemical property of the sample was determined by the XPS technique. The survey and core level spectra for Ti 2p and O 1s are given in Figures 3(d)–3(f). Ti 2p signals consist of the well distinct Ti 2p<sub>1/2</sub> and Ti 2p<sub>3/2</sub> peaks located at 464.5 and 458.5 eV, respectively. In the O 1s spectrum, there appears a strong signal at around 530.2 eV accompanied by a shoulder at 531.7 eV which originates from the crystalline oxygen (O<sup>2-</sup>) and the surface-adsorbed oxygen, respectively [26].

The photocatalytic property of the as-prepared brookite TiO<sub>2</sub> was evaluated by the degradation of an MO solution under UV light. Figure 4(a) shows the degradation rate of MO with and without the sample under UV light. As we

can see, brookite TiO<sub>2</sub> exhibits photocatalytic activity with an efficiency of nearly 85% in 3 h, which is relatively lower than previously reported [9, 27]. Photocatalysis and photoluminescence are two competitive processes of photoinduced carriers, and low photocatalytic activity often results from high band-to-band photoluminescent efficiency [28]. Figure 4(b) shows the photoluminescence spectrum excited at 310 nm. Two main emission peaks appear at about 410 and 464 nm wavelengths, respectively. The former is attributed to band-band photoluminescence, and the latter is attributed to the transition between impurity and valence energy levels [28]. Moreover, ESR spin-trapping analysis was employed to probe the active species. As shown in Figure 4(c), it is observed that four characteristic 1:2:2:1 quadruple peaks of DMPO-OH show a slow augmentation with UV-light irradiation. According to the above investigations, the photocatalytic and photoluminescent mechanisms of brookite TiO<sub>2</sub> are proposed in Figure 4(d). When TiO<sub>2</sub> is

irradiated with light with an energy higher or equal to the band gap energy, electrons are excited to the conduction band with the simultaneous generation of holes ( $h^+$ ) in the valence band. The separation and recombination of photoinduced charge carriers are competitive processes, which produce the photocatalytic reaction and photoluminescent process, respectively.

#### 4. Conclusions

In summary, high-purity brookite-type  $\text{TiO}_2$  nanomaterials were prepared by regulating the reaction time using titanium sulfate as the titanium source and chloroacetic acid as the surface active agent under hydrothermal conditions. With the prolongation of the hydrothermal reaction time, the originally formed anatase-phase  $\text{TiO}_2$  gradually transformed into the brookite phase, and a high-purity brookite sample was obtained when the hydrothermal reaction time was prolonged to 9 h. TEM characterization found that the as-prepared brookite  $\text{TiO}_2$  exhibited a hollow-sphere morphology self-assembled by nanoblocks. The surface of the brookite  $\text{TiO}_2$  sample was capped by water and other organic molecules, as indicated by FT-IR and TG-DTA results. The photocatalytic and photoluminescent properties of the brookite  $\text{TiO}_2$  hollow spheres were investigated for the first time. The reported findings will be greatly useful in phase and morphology regulation of titanium dioxide.

#### Data Availability

The findings of this study are available from the corresponding author upon request. The public database is not used in this article.

#### Conflicts of Interest

The authors declare that there is no conflict of interests regarding the publication of this paper.

#### Acknowledgments

This work was financially supported by the Educational Committee of the Natural Science Foundation of Anhui Province (No. KJ2017A386) and the Anhui Provincial Innovation Team of Design and Application of Advanced Energetic Materials (KJ2015TD003).

#### References

- [1] L. B. Xiong, J. L. Li, B. Yang, and Y. Yu, " $\text{Ti}^{3+}$  in the surface of titanium dioxide: generation, properties and photocatalytic application," *Journal of Nanomaterials*, vol. 2012, Article ID 831524, 13 pages, 2012.
- [2] Y. Zou, X. Tan, T. Yu, Y. Li, Q. Shang, and W. Wang, "Synthesis and photocatalytic activity of chrysanthemum-like brookite  $\text{TiO}_2$  nanostructures," *Materials Letters*, vol. 132, pp. 182–185, 2014.
- [3] G. Li, L. Li, J. Boerio-Goates, and B. F. Woodfield, "High purity anatase  $\text{TiO}_2$  nanocrystals: near room-temperature synthesis, grain growth kinetics, and surface hydration chemistry," *Journal of the American Chemical Society*, vol. 127, no. 24, pp. 8659–8666, 2005.
- [4] J. M. Johnson, N. Kinsinger, C. Sun, D. Li, and D. Kisailus, "Urease-mediated room-temperature synthesis of nanocrystalline titanium dioxide," *Journal of the American Chemical Society*, vol. 134, no. 34, pp. 13974–13977, 2012.
- [5] D. Machon, M. Daniel, V. Pischedda, S. Daniele, P. Bouvier, and S. LeFloch, "Pressure-induced polyamorphism in  $\text{TiO}_2$  nanoparticles," *Physical Review B*, vol. 82, no. 14, article 140102, 2010.
- [6] J. Yu, J. Low, W. Xiao, P. Zhou, and M. Jaroniec, "Enhanced photocatalytic  $\text{CO}_2$ -reduction activity of anatase  $\text{TiO}_2$  by coexposed {001} and {101} facets," *Journal of the American Chemical Society*, vol. 136, no. 25, pp. 8839–8842, 2014.
- [7] H. Chen, C. E. Nanayakkara, and V. H. Grassian, "Titanium dioxide photocatalysis in atmospheric chemistry," *Chemical Reviews*, vol. 112, no. 11, pp. 5919–5948, 2012.
- [8] S. Selcuk and A. Selloni, "Facet-dependent trapping and dynamics of excess electrons at anatase  $\text{TiO}_2$  surfaces and aqueous interfaces," *Nature Materials*, vol. 15, no. 10, pp. 1107–1112, 2016.
- [9] H. Lin, L. Li, M. Zhao et al., "Synthesis of high-quality brookite  $\text{TiO}_2$  single-crystalline nanosheets with specific facets exposed: tuning catalysts from inert to highly reactive," *Journal of the American Chemical Society*, vol. 134, no. 20, pp. 8328–8331, 2012.
- [10] M. Choi and K. Yong, "A facile strategy to fabricate high-quality single crystalline brookite  $\text{TiO}_2$  nanoarrays and their photoelectrochemical properties," *Nanoscale*, vol. 6, no. 22, pp. 13900–13909, 2014.
- [11] J. Pan and S. P. Jiang, "Synthesis of nitrogen doped faceted titanium dioxide in pure brookite phase with enhanced visible light photoactivity," *Journal of Colloid and Interface Science*, vol. 469, pp. 25–30, 2016.
- [12] D. Dambournet, I. Belharouak, and K. Amine, "Tailored preparation methods of  $\text{TiO}_2$  anatase, rutile, brookite: mechanism of formation and electrochemical properties," *Chemistry of Materials*, vol. 22, no. 3, pp. 1173–1179, 2010.
- [13] R. Kaplan, B. Erjavec, G. Dražić, J. Grdadolnik, and A. Pintar, "Simple synthesis of anatase/rutile/brookite  $\text{TiO}_2$  nanocomposite with superior mineralization potential for photocatalytic degradation of water pollutants," *Applied Catalysis B: Environmental*, vol. 181, pp. 465–474, 2016.
- [14] M. Altomare, M. V. Dozzi, G. L. Chiarello, A. di Paola, L. Palmisano, and E. Selli, "High activity of brookite  $\text{TiO}_2$  nanoparticles in the photocatalytic abatement of ammonia in water," *Catalysis Today*, vol. 252, pp. 184–189, 2015.
- [15] X. Zhao, B. M. Sánchez, P. J. Dobson, and P. S. Grant, "The role of nanomaterials in redox-based supercapacitors for next generation energy storage devices," *Nanoscale*, vol. 3, no. 3, pp. 839–855, 2011.
- [16] J. G. Li, T. Ishigaki, and X. Sun, "Anatase, brookite, and rutile nanocrystals via redox reactions under mild hydrothermal conditions: phase-selective synthesis and physicochemical properties," *Journal of Physical Chemistry C*, vol. 111, no. 13, pp. 4969–4976, 2007.
- [17] K. Sabyrov, N. D. Burrows, and R. L. Penn, "Size-dependent anatase to rutile phase transformation and particle growth," *Chemistry of Materials*, vol. 25, no. 8, pp. 1408–1415, 2013.
- [18] H. Yan, P. Song, S. Zhang, Z. Yang, and Q. Wang, "Facile fabrication and enhanced gas sensing properties of hierarchical

- MoO<sub>3</sub> nanostructures,” *RSC Advances*, vol. 5, no. 89, pp. 72728–72735, 2015.
- [19] R. Bleta, P. Alphonse, and L. Lorenzato, “Nanoparticle route for the preparation in aqueous medium of mesoporous TiO<sub>2</sub> with controlled porosity and crystalline framework,” *Journal of Physical Chemistry C*, vol. 114, no. 5, pp. 2039–2048, 2010.
- [20] Q. Xu, J. Zhang, Z. Feng, Y. Ma, X. Wang, and C. Li, “Surface structural transformation and the phase transition kinetics of brookite TiO<sub>2</sub>,” *Chemistry - An Asian Journal*, vol. 5, no. 10, pp. 2158–2161, 2010.
- [21] W. Tong, L. Li, W. Hu, T. Yan, and G. Li, “Systematic control of monoclinic CdWO<sub>4</sub> nanophase for optimum photocatalytic activity,” *Journal of Physical Chemistry C*, vol. 114, no. 3, pp. 1512–1519, 2010.
- [22] W. Hu, L. Li, G. Li, C. Tang, and L. Sun, “High-quality brookite TiO<sub>2</sub> flowers: synthesis, characterization, and dielectric performance,” *Crystal Growth & Design*, vol. 9, no. 8, pp. 3676–3682, 2009.
- [23] J. C. Yu, L. Zhang, and J. Yu, “Direct sonochemical preparation and characterization of highly active mesoporous TiO<sub>2</sub> with a bicrystalline framework,” *Chemistry of Materials*, vol. 14, no. 11, pp. 4647–4653, 2002.
- [24] V. M. Huxter, T. Mirkovic, P. S. Nair, and G. D. Scholes, “Demonstration of bulk semiconductor optical properties in processable Ag<sub>2</sub>S and EuS nanocrystalline systems,” *Advanced Materials*, vol. 20, no. 12, pp. 2439–2443, 2008.
- [25] M. Monai, T. Montini, and P. Fornasiero, “Brookite: nothing new under the sun?,” *Catalysts*, vol. 7, no. 10, p. 304, 2017.
- [26] K. S. Kim and N. Winograd, “X-ray photoelectron spectroscopic studies of nickel-oxygen surfaces using oxygen and argon ion-bombardment,” *Surface Science*, vol. 43, no. 2, pp. 625–643, 1974.
- [27] J. Zhang, P. Zhou, J. Liu, and J. Yu, “New understanding of the difference of photocatalytic activity among anatase, rutile and brookite TiO<sub>2</sub>,” *Physical Chemistry Chemical Physics*, vol. 16, no. 38, pp. 20382–20386, 2014.
- [28] J. Liqiang, Q. Yichun, W. Baiqi et al., “Review of photoluminescence performance of nano-sized semiconductor materials and its relationships with photocatalytic activity,” *Solar Energy Materials and Solar Cells*, vol. 90, no. 12, pp. 1773–1787, 2006.



**Hindawi**  
Submit your manuscripts at  
[www.hindawi.com](http://www.hindawi.com)

